Identification of novel *Fgf* enhancers and their role in dental evolution

Vagan Tapaltsyan[1], **Cyril Charles**[1,2], **Jianxin Hu**[3], **David Mindell**[4], **Nadav Ahituv**[5,6], **Gregory M. Wilson**[7], **Brian L. Black**[3], **Laurent Viriot**[2], and **Ophir D. Klein**[1,6,8,*]

[1]Department of Orofacial Sciences and Program in Craniofacial and Mesenchymal Biology, University of California San Francisco, San Francisco, California 94143, USA

[2]Team «Evo-Devo of Vertebrate Dentition», Institut de Génomique Fonctionnelle de Lyon, ENS de Lyon, Université de Lyon, Université Lyon 1, CNRS, Ecole Normale Supérieure de Lyon, Lyon, France

[3]Cardiovascular Research Institute, University of California San Francisco, San Francisco, CA, 94158, USA

[4]Division of Environmental Biology, National Science Foundation, Arlington, Virginia, 22230, USA

[5]Department of Bioengineering and Therapeutic Sciences, University of California San Francisco, California, 94158, USA

[6]Institute for Human Genetics, University of California San Francisco, San Francisco, California, 94143, USA

[7]Department of Biology, University of Central Oklahoma, Edmond, Oklahoma, 73034, USA

[8]Department of Pediatrics, University of California San Francisco, San Francisco, California 94143, USA

Abstract

Mammalian dental morphology is under strong evolutionary pressure because of its importance for mastication and diet. While the mechanisms underlying tooth development have been widely studied in model organisms, the role of genetic regulatory elements in patterning the different elements of the occlusal surface and crown height across species is not well understood. Previous studies showed that Fibroblast Growth Factor (FGF) genes are important regulators of tooth development that influence morphological variation. We hypothesized that interspecific variation in rodent dental morphology could be governed by nucleotide variation in genetic regulatory elements that modulate the spatial and temporal expression of the genes encoding FGF signalling molecules. In this study, we compared the variation in dental morphology across nine taxa of rodents to the variation in sequences of non-coding evolutionary conserved regions (ECRs) of *Fgf3, 4, 8, 9,* and *10.* We correlated the variation in molar tooth cusp shape and the evolution of high molar crowns (hypsodonty) to the patterns of sequence variation in two ECRs, *Fgf10ECR3* and *Fgf9ECR1*, respectively. By conducting luciferase and electrophoretic mobility shift assays,

*Corresponding author: Ophir Klein, University of California, San Francisco, 513 Parnassus Ave, HSE1509, San Francisco, CA, USA 94143, Phone: +1-415-476-4719, Fax: +1-415-476-9513, ophir.klein@ucsf.edu.

we determined that these ECRs could function as enhancers. These data suggest that emergence of hypsodonty and occlusal cusp patterning may have happened through the evolutionary changes in enhancers, such as *Fgf9ECR1* and *Fgf10ECR3,* which affected the expression of major signaling molecules involved in tooth development.

INTRODUCTION

The origin of species by means of natural selection is dependent upon the intra-specific variation of traits, which are genetically encoded. These traits can present in the form of derived physical phenotypes that emerge through novel changes in the genome under selective pressures. An important adaptation to changing niches and expansion into new adaptive zones is the evolution of traits associated with foraging behavior (Heard and Hauser, 1995). The ability to consume a wider range of foods includes changes in both behavioral and physical phenotypes. Thus, investigation of the evolution of traits associated with foraging can provide much insight about the interplay between morphological variability and evolution.

One example of such evolutionary processes is the emergence of variation in traits associated with mastication (chewing). Rodents occupy a diverse range of ecological niches, from cold and hot deserts to rainforests. This range is associated with varied food resources and diverse diets. One constant morpho-functional character of all rodents is to gnaw using their continuously growing incisors, but their postcanine dentition (*i.e.* premolars and molars) may show very different dental morphologies from one species to another. During their evolution, some rodent lineages modified their diet from omnivorous to more specialized diets, such as granivory or herbivory (Rodrigues et al., 2009). These specializations were made possible by modifications of the dental morphology.

In many rodent lineages, two general strategies, which aim at increasing the surface area of mastication and/or the longevity of the tooth function, are observed. First, the occlusal surface area for grinding and crushing food can be increased by adding additional cusps, which can afterwards become more effective at mastication by merging together into lophs (Janis and Fortelius, 1988). Second, extending the duration of growth, leading to increased dental crown height, can increase the longevity of postcanine teeth. Most rodents have postcanine teeth with limited growth (brachydont teeth), characterized by low crowns that fully emerge from the jawbone when they are functional. However, some rodents have evolved postcanine teeth with extended growth (hypsodont teeth), characterized by higher crowns that are partially encased in the bone and continue erupting as the tooth becomes progressively worn over the course of the animal's life (Fig. 1A). In extreme cases, hypsodonty can lead to crowns that continuously grow over the animal's life without developing roots, referred to as euhypsodonty (Koenigswald and Clemens, 1992). In this manuscript, we will use the term 'hypsodonty' *sensu lato*, including euhypsodonty, in its definition.

Most studies dealing with evolutionary developmental biology of the dentition in mammals have used the laboratory mouse (*Mus musculus*) as a model. The mouse has a postcanine dentition made only of brachydont molars, as the premolars were lost in the course of

evolution (Jernvall and Jung, 2000). To address the question of molar growth duration, mouse molars are often compared to the continuously growing molars of the sibling vole (*Microtus levis*). Decreased *Fgf3* dosage in mice and humans caused reductions in cusp number and changes in dental morphology that mimicked the ancestral conditions found in fossil murine rodents and early anthropoid primates, respectively (Charles et al., 2009). In contrast, gain of function of ectodysplasin (Eda) and its receptor (Edar) is thought to have modified the dental pattern with the development of new crests (Rodrigues et al., 2013). Further, *Fgf10* expression ceased at embryonic day (E) 17 in developing brachydont mouse molars but persisted in hypsodont vole molars (Tummers and Thesleff, 2003). Moreover, *in vitro* activation of *Fgf10* in developing mouse molars resulted in higher cusps (Yokohama-Tamaki et al., 2006). Thus, the elongation of the dental occlusal surface by the addition of neoformed cusps, as well as the extension of the growth duration of the crown, may have evolved through mechanisms that resulted in temporal changes in expression of genes involved in morphogenesis.

The FGF signaling pathway mediates epithelial-mesenchymal interactions at several stages of tooth morphogenesis in mammals and other vertebrates (Jackman et al., 2004; Mandler and Neubuser, 2001). In developing mouse molars, at least ten different FGF ligands (FGF3, 4, 8, 9, 10, 15, 16, 17, 18, and 20) are expressed in complex, overlapping patterns in the epithelium and/or mesenchyme (Jernvall et al., 2000; Keranen et al., 1999; Kettunen and Thesleff, 1998; Li et al., 2014). While the precise roles of FGF3, 4, 8, 9, and 10 in tooth development have been largely described, the role of other ligands requires further investigation (Li et al., 2014). Although variations in the coding sequences of genes can lead to changes in morphology, differences in non-coding DNA sequences, such as the enhancers that regulate gene expression, may also contribute to such variations by altering the spatial and temporal expression patterns (King and Wilson, 1975; Visel et al., 2009). To investigate the evolutionary role of FGF genes implicated in determination of tooth number and morphology, we compared the variation of the non-coding evolutionary conserved regions (ECRs) found within 0.5 megabases of *Fgf3, 4, 8, 9,* and *10*. We then sequenced the identified ECRs in nine species of rodents representing different ecological niches and correlated ECR sequence diversity to the patterns of dental morphology variation. Finally, we determined to what extent the ECRs that correlated to variation of a certain dental character state could function as enhancers by identifying transcription factor binding sites (TFBSs) within the ECR sequences and utilizing luciferase assays and electrophoretic mobility shift assays (EMSAs).

MATERIALS AND METHODS

Examination of specimens

Museum specimen skulls were obtained from the California Academy of Sciences, University of Central Oklahoma Museum of Vertebrates, and the National Natural History Museum of Paris. Teeth were visualized using a Leica M205C dissection microscope. Dental rows of three species belonging to the superfamily Muroidea, *Lemmus lemmus* (Arviolinae), *Ondatra zibethicus* (Arviolinae), and *Mus musculus* (Murinae), were imaged by X-ray cone-beam microtomography using a Nanotom (GE) at an energy of 100keV to illustrate the

morphological differences between brachydont and hypsodont molars. All 3D renderings were done using VGStudiomax 2.2 software.

ECR identification and amplification

Genomic DNA from the nine species of examined rodents was extracted and purified via phenol/chloroform from muscle tissues obtained from the California Academy of Sciences and University of Central Oklahoma. We utilized five representatives for each species (n=5). Primers were designed based on *Mus-Xenopus* sequence variation (Table S2). The ECRs were amplified for all nine species and one outgroup [*Mephitis mephitis* (skunk)] via PCR by using standard procedures and were sequenced with ABI3130xl Genetic Analyzer. Sequence data were analyzed in Geneious 8.1. We calculated percent sequence divergence as average percentage of sequence variation among examined genetic variants (Gojobori et al., 1990) and built neighbor-joining trees for each ECR in Geneious 8.1 (Kearse et al., 2012).

Comparative analysis of identified ECRs

Sequence divergence of each ECR, illustrated by neighbor-joining trees, was compared against the dental morphology diversity in all examined rodent species. Only interspecific monophyletic groups with 100% of the members exhibiting the same dental character phenotype were selected.

Transcription factor binding site analysis

Sequences of *Fgf9ECR1a*, *Fgf9ECR1b*, *Fgf10hypso+*, and *Fgf10hypso−* were input into the rVista2.0 Mulan TFBS locator (Loots and Ovcharenko, 2004). TRANSFAC V10.2 library, containing 467 unique TBFS sequences was used. Matrix similarity was set to 0.95. Sequence similarity was confirmed in JASPAR (Mathelier et al., 2014; Portales-Casamar et al., 2010).

Luciferase assay

Sequences of *Fgf9ECR1a*, *Fgf9ECR1b*, *Fgf10hypso+*, and *Fgf10hypso−* were inserted into the *Kpn*I and *Hind*III sites in the pGL3-enhancer reporter vector (Promega). Mouse ameloblast-derived LS8 cells were cultured in DMEM with 10% FBS at 37°C and 5% CO_2. Cells (1×10^5) were plated in 35mm plates. Each transfection was standardized for 0.5 μg of expression vector, 1 μg luciferase reporter vector, and 1 μg pTK-Renilla vector. Fugene (3 μl) and plasmids were mixed in 97 μl DMEM (Invitrogen). The mixture was incubated for 20 min at room temperature and added to the cells. The cells were cultured for 48 h, lysed and measured for luciferase activity by Dual-Glo Luciferase Assay System (Promega) standard protocol in a Glomax Luminometer (Promega). The *Renilla* luciferase vector was used for normalization. Assays were carried out to achieve n=3. Differences in luminescence level and standard deviation were calculated and significance was evaluated by student's t-test (Sherf, 1996).

Quantitative real-time PCR

Six lower molars were dissected from E15 wild-type (wt) mice and pooled. Cervical loops were dissected from postnatal day (P) 30 wt mice. LS8 cells were grown to confluence in

three 35 mm plates (~3×10^6 cells), resuspended, and combined. Samples were placed into 350 μl RNeasy lysis buffer (Qiagen). Samples were DNase-treated and standardized to 350 ng of DNA. Reverse transcription was carried out with Multireverse Transcriptase (New England Biolabs), and quantitative PCR was performed. Expression was normalized to *L19* expression. All assays were performed at least three times. Standard deviation was calculated. See Table S2 for primer list.

Electrophoretic mobility shift assay

EMSAs were carried out with recombinant proteins synthesized in *Escherichia coli* (*E. coli*). Control (labeled) and ECR (cold inhibitor) oligonucleotides were annealed in a thermocycler (Eppendorf) (see Table S2 for list of primers). Control oligonucleotides were labeled with [γ-^{32}P]rATP utilizing T4 polynucleotide kinase and purified. EMSA master mixes included 40,000 cpm (~0.2 ng double stranded oligonucleotide probe) and 10 μg of nuclear protein in a final volume of 15 μl of 4% glycerol; 1 mM $MgCl_2$; 0.5 mM DTT; 50 mM NaCl; 10 mM Tris–HCl, and 1 μg of poly (dI-dC). The mixes were incubated for 20 min at room temperature, following 10 min incubation with addition of cold competitor ECR in molar excess and 20 min incubation with addition of the labeled probe. Finally, mixtures were incubated for 30 min in the presence of commercial anti-peptide antibodies (Sigma and Abcam). The reaction mixtures were loaded onto 6% native polyacrylamide gels and electrophoresed at 250 V for 2–3 hours. The gels were then dried and subjected to autoradiography.

RESULTS

Comparative anatomy of rodent teeth

We began by examining the morphology of the molar teeth of rodents belonging to the following families: Heteromyidae, *Dipodomys ordii* (Dipodomyinae), *Chaetodipus hispidis* (Perognathinae); Dipodidae, *Napaeozapus insignis* (Zapodinae); Cricetidae, *Microtus californicus* (Arvicolinae), *Neotoma micropus* (Neotominae), *Peromyscus maniculatus* (Neotominae); and Muridae, *Acomys cahirinus* (Deomyinae), *Lophuromys flavopunctatus* (Deomyinae), *Mus musculus* (Murinae). Within this group, only the Heteromyidae and sometimes the Dipodidae have premolars associated with the molars (Kays and Wilson, 2009). All of the other species are Muroidea and only have molar and incisor teeth. These species were chosen to cover a wide range of dental phenotypes and geographical repartition (Fig. 1 and S1) (Kays and Wilson, 2009; Wilson and Reeder, 2005).

Identification and characterization of FGF ECRs

Since the genomes for the majority of examined species have not been sequenced, we took a comparative approach to identify ECRs for *Fgf3, 4, 8, 9,* and *10* for each species. First, we utilized the ECR Browser (http://ecrbrowser.dcode.org) to identify ECRs among mouse (*Mus*), rat (*Rattus*), and frog (*Xenopus*) up to 0.5 megabases upstream and downstream of the promoter region for each gene (Loots and Ovcharenko, 2004; Visel et al., 2009). We selected ECRs of >100 base pairs (bp) in length that exhibited at least 75% sequence identity between *Mus* and *Xenopus* and 90% sequence identity between *Mus* and *Rattus*. The rationale behind this approach was that if any particular ECR exhibited high conservation

and apparent homology between *Mus* and *Xenopus*, it could have a functional role, such as serving as a regulatory element, and would also likely be conserved among all nine species of rodents used in this study.

We focused on proximal-acting enhancers, limiting our search to 0.5 megabases upstream and downstream of the promoter regions of *Fgf3, 4, 8, 9,* and *10*. A total of seven ECRs were identified (Fig. S2). Conserved regions exhibited at least 95% sequence identity between Mus and *Rattus* and at least 75% sequence identity between *Mus* and *Xenopus*. The identified ECRs for *Fgf3* and *4* exhibited 100% sequence identity among all 9 species, whereas ECRs for *Fgf8, 9,* and *10* exhibited 9.6–11.5% sequence variation among the examined species (Table S1).

Correlation of *Fgf9ECR1* and *Fgf10ECR3* sequence identity and dental phenotype variation

We next asked if the sequence identity of the identified ECRs corresponded to the patterns of dental character variation among the 9 species of rodents. We identified a significant correlation between the sequence variant diversity of *Fgf10ECR3* and the brachydont/hypsodont molar diversity in all nine species. We established the correlations by constructing neighbor-joining trees to estimate relationship based on *Fgf10ECR3* sequence and compared it among the species in respect to the molar height phenotype. We identified a group of closely related *Fgf10ECR3* sequences found only in hypsodont species, while the rest of the sequences were associated with brachydont species (Fig. 2A,C). We thus termed those sequences *Fgf10ECR3hypso+* and *Fgf10ECR3hypso−,* respectively. We then compared the sequence diversity to previously reported phylogenetic studies of the examined rodent species (Fig. 2B) (Fabre et al., 2012). The monophyletic distribution of hypsodont clades based on *Fgf10ECR3* sequence neighbor-joining tree, contrasted with the published phylogenies for species we studied (Fabre et al., 2012) supports the idea that emergence of hypsodonty was a very dynamic evolutionary process (Fig. 2B).

In contrast, *Fgf9ECR1* displayed a lack of correlation between sequence and dental morphological characteristics among the species examined (Fig. 3A,C). Interestingly, two of the Muroidea species examined here, *Microtus californicus* and *Neotoma micropus*, share the same *Fgf9ECR1b* sequence associated with 'triangular' shape of the cusps (marked with asterisk), but they have distinct occlusal morphologies (Fig. 3C). The triangular cusped clade monophyletic distribution based on the *Fgf9ECR1* sequence also differed from the paraphyletic distribution in the neighbor-joining tree based on mitochondrial DNA sequence data, further supporting the convergent nature of the ECR sequence and phenotype acquisition (Fig 3A,B). Therefore, we decided to compare one muroid with the *Fgf9ECR1a* variant (*Mus musculus*) to one muroid with the *Fgf9ECR1b* variant (*Neotoma micropus*). No correlation was found for *Fgf8ECR1, Fgf10ECR1,* and *Fgf10ECR2* (Fig. S4 and Table S1), as no single dental characteristic matched any of the ECR sequence variants.

ECR functional enhancer assays

Based on our observations that *Fgf10ECR3* showed a correlation between sequence variation and tooth morphology while *Fgf9ECR1* did not show the same correlation, we decided to investigate whether either of these ECR sequences (Fig. 4) might function as

transcriptional enhancers. We examined the *Fgf9ECR1 and Fgf10ECR3* sequences of *Mus musculus* (brachydont, rounded cusps) and *Microtus californicus* (hypsodont, triangular cusps) for conserved, putative transcription factor binding sites. Interestingly, we discovered that the sequence variation between Fgf9ECR1 and Fgf10ECR3 variants resulted in additional potential binding sites for the transcription factors PAX4 and VDR in *Fgf9ECR1a* (*Mus*) sequence and BACH2, MSX1, PAX3, PAX8, and GATA8 in *Fgf10ECR3hypso+* (*Microtus*) sequence (Fig. 4).

To assess if the presence of those binding sites could be relevant for tooth development, we investigated the expression of the transcription factors in dental tissues and derived cell lines (Fig. 5). Previous studies have revealed that many of the same signaling molecules expressed in the adult mouse incisor cervical loop and in vole molar intercuspal loops are extinguished by later stages of mouse molar development, we conducted rt-PCR in E15 developing mouse molar, adult incisor, and LS8 dental cell line. *Bach2*, *Msx1*, *Pax3*, *Pax4*, and *Gata4* were expressed in both developing mouse molar and adult cervical loop, and most of the transcription factors were also expressed in the LS8 cell line (Fig. 5A). This suggested a general functional significance of the TFs in all dental tissues.

Because the sequence variation between the putative enhancers for *Fgf9* and *Fgf10* resulted in a gain of TFBSs for *Fgf9ECR1a* (absent in *Fgf9ECR1b*) and *Fgf10ECR3hypso+* (absent in *Fgf10ECR3hypso−*), we selected three such TFs (GATA4, MSX1, and PAX4) to determine their capacity for preferential interaction with ECRs by conducting EMSA (Fig. 5B). We incubated the peptides in the presence of *Fgf9ECR1a, Fgf9ECR1b, Fgf10ECR3hypso+,* and *Fgf3ECR1hypso−*. We observed binding of the ^{32}P-labeled positive control probes to the transcription factors, resulting in a shift in the band position. Furthermore, we introduced antibodies against the TFs and observed a super-shift, reflecting the probe/peptide/antibody complex. In all cases, introduction of the unlabeled *Fgf9ECR1a* and *Fgf10ECR3hypso+* oligonucleotides resulted in a lack of bands, signifying competition of the ECRs with the probe, while introduction of the unlabeled *Fgf9ECR1b* and *Fgf10ECR3hypso−* did not result in competition. These results indicate that *Fgf9ECR1a* and *Fgf10ECR3hypso+* are capable of outcompeting *Fgf9ECR1b* and *Fgf10ECR3hypso−* in binding of the TF and TF/antibody complexes.

Finally, to test for possible transcriptional enhancer function of *Fgf9ECR1* and *Fgf10ECR3*, we conducted luciferase assays in the ameloblast-derived LS8 cell line (Fig. 5B). The *Mus* and *Microtus Fgf9ECR1* and *Fgf10ECR3* were inserted upstream of the promoter sequence in luciferase-containing pGL3-enhancer vector plasmids, and luciferase activity was determined (Fig. 5C). The plasmids with inserted *Mus* and *Microtus Fgf9ECR1* and *Fgf10ECR3* sequences were transfected into the cells and enhancer function was estimated. While both sequence variants of *Fgf9ECR1* and *Fgf10ECR3* exhibited higher luminescence output than the control (empty vector), insertion of *Fgf9ECR1a* and *Fgf10ECR3hypso+* resulted in significantly higher levels of luciferase expression than *Fgf9ECR1b* and *Fgf10ECR3hypso−* and thus exhibited stronger enhancer function (Fig. 5C).

DISCUSSION

Variation in enhancer sequences is a powerful mechanism for evolution of novel phenotypes, as small sequence changes can result in profoundly different patterns of gene expression (Cretekos et al., 2008; Prud'homme et al., 2007). Tooth development relies on complex interactions between several major signaling pathways that underlie the crosstalk between the epithelium and the underlying mesenchyme (Thesleff, 2003). Thus, alterations in the expression level or pattern of a single molecule in these complex interactions could lead to phenotypic changes.

Chromatin-based enhancer identification assays, such as p300 ChIP-seq experiments, present unbiased whole-genome data, but their use is largely limited to species with available genomes (Blow et al., 2010). Here, we took a comparative approach to identification and characterization of novel putative enhancer regions for several FGF genes that have been previously reported to be involved in tooth development (Charles et al., 2009; Harada et al., 2002; Kettunen et al., 2000; Kettunen and Thesleff, 1998). By loosening the parameters for inter-class (distal) conservation (mouse-frog) to 75% but maintaining proximal inter-genus conservation (mouse-rat) at 95%, we sought to capture evolutionarily important ECRs with a potential for novel functions in rodents. This approach allowed us to identify such regions and to sequence them for all of the non-model rodent species in the study. Further, by comparing the ECR variation data to specific phenotypic variation data among the selected species, we were able to select candidates for functional investigation.

The comparative approach pointed to three types of ECRs. First, we identified ECRs of *Fgf3* and *4* as having no sequence variation (were fully conserved) among all examined rodent species. Such high levels of conservation suggest functional significance, although it is unknown in which organ and what stage of development such sequences would be important (Halligan et al., 2013). While such high conservation does not allow for comparative studies, these ECRs are good candidates for future investigation as regulatory elements, such as transgenic approaches for the *in vivo* investigation of the spatial and temporal range of the candidate enhancers, as well as functional genetic manipulation and substitution of enhancers in a mouse model. Second, we identified a number of ECRs for *Fgf8* and *10* that exhibited variation among the examined species. However, intersection of the molecular and morphologic data did not identify a correlation with any specific dental phenotype. The third group of identified ECRs, *Fgf9ECR1* and *Fgf10ECR3*, exhibited sequence variation that was correlated to the variation of cusp shape within Muroidea and hypsodonty, respectively. Such correlation led us to further pursue the functional characterization of two of these ECRs. We identified several putative transcription factor binding sites in the *Fgf9ECR1a* and *Fgf10ECR3hypso+* sequences and determined that those variants are capable of promoting higher levels of gene expression than their counterparts in a cell culture system. Specifically, the sequence variation resulting in a gain of TF binding sites in some of the examined species provided for an experimental model where nature itself had provided both TFBS sequences and also mutated sequences. Thus, we were able to show that these TFs may regulate the expression of *Fgf9* and *Fgf10* by binding to *Fgf9ECR1* and *Fgf10ECR3,* as *Fgf9ECR1a* and *Fgf10ECR3hypso+* exhibited stronger enhancer function in systems where the aforementioned TFs were expressed.

Comparative expression studies between mice and voles have shown similarities in gene expression patterns during early stages of tooth development (Keranen et al., 1998). However, many signaling molecules whose expression decreases at later stages of mouse molar development persist in vole molars (Keranen et al., 1998). For example, as previously mentioned, the expression of *Fgf10* in vole molars persists after E17. Moreover, continuous expression of *Fgf10* is required for continuous growth of the incisor. Prolonged expression of *Fgf10* in the dental mesenchyme resulted in higher crowns (Yokohama-Tamaki et al., 2006). Similarly, *Fgf9* is expressed in the secondary enamel knots, which correspond to the sites of future cusps (Kettunen and Thesleff, 1998). Thus, it may be that spatial and temporal variation of *Fgf9* expression can result in cusp modification. A plausible evolutionary mechanism for changing the pattern of the expression of *Fgf9* and *10* in developing molars may be through sequence alterations within evolutionarily conserved regions, resulting in spatial and temporal gain of enhancer function, such as the case of *Fgf9ECR1a* and *Fgf10ECR3hypso+*.

Supplementary Material

Refer to Web version on PubMed Central for supplementary material.

Acknowledgments

References

Blow MJ, McCulley DJ, Li Z, Zhang T, Akiyama JA, Holt A, Plajzer-Frick I, Shoukry M, Wright C, Chen F, et al. ChIP-Seq identification of weakly conserved heart enhancers. Nat Genet. 2010; 42:806–810. [PubMed: 20729851]

Charles C, Lazzari V, Tafforeau P, Schimmang T, Tekin M, Klein O, Viriot L. Modulation of Fgf3 dosage in mouse and men mirrors evolution of mammalian dentition. Proceedings of the National Academy of Sciences of the United States of America. 2009; 106:22364–22368. [PubMed: 20018768]

Cretekos CJ, Wang Y, Green ED, Martin JF, Rasweiler JJt, Behringer RR. Regulatory divergence modifies limb length between mammals. Genes & development. 2008; 22:141–151. [PubMed: 18198333]

Fabre PH, Hautier L, Dimitrov D, Douzery EJ. A glimpse on the pattern of rodent diversification: a phylogenetic approach. BMC evolutionary biology. 2012; 12:88. [PubMed: 22697210]

Gojobori T, Moriyama EN, Kimura M. Statistical methods for estimating sequence divergence. Methods in enzymology. 1990; 183:531–550. [PubMed: 2314291]

Halligan DL, Kousathanas A, Ness RW, Harr B, Eory L, Keane TM, Adams DJ, Keightley PD. Contributions of protein-coding and regulatory change to adaptive molecular evolution in murid rodents. PLoS Genet. 2013; 9:e1003995. [PubMed: 24339797]

Harada H, Toyono T, Toyoshima K, Ohuchi H. FGF10 maintains stem cell population during mouse incisor development. Connect Tissue Res. 2002; 43:201–204. [PubMed: 12489159]

Heard S, Hauser D. Key evolutionary innovations and their ecological mechanisms. Historical Biology. 1995; 10:151–173.

Jackman WR, Draper BW, Stock DW. Fgf signaling is required for zebrafish tooth development. Dev Biol. 2004; 274:139–157. [PubMed: 15355794]

Janis CM, Fortelius M. On the means whereby mammals achieve increased functional durability of their dentitions, with special reference to limiting factors. Biol Rev Camb Philos Soc. 1988; 63:197–230. [PubMed: 3042033]

Jernvall J, Jung HS. Genotype, phenotype, and developmental biology of molar tooth characters. Am J Phys Anthropol Suppl. 2000; 31:171–190.

Jernvall J, Keranen SV, Thesleff I. Evolutionary modification of development in mammalian teeth: quantifying gene expression patterns and topography. Proceedings of the National Academy of Sciences of the United States of America. 2000; 97:14444–14448. [PubMed: 11121045]

Kays, R.; Wilson, D. Mammals of North America. 2. Princeton Press; 2009.

Kearse M, Moir R, Wilson A, Stones-Havas S, Cheung M, Sturrock S, Buxton S, Cooper A, Markowitz S, Duran C, et al. Geneious Basic: an integrated and extendable desktop software platform for the organization and analysis of sequence data. Bioinformatics. 2012; 28:1647–1649. [PubMed: 22543367]

Keranen SV, Aberg T, Kettunen P, Thesleff I, Jernvall J. Association of developmental regulatory genes with the development of different molar tooth shapes in two species of rodents. Dev Genes Evol. 1998; 208:477–486. [PubMed: 9799429]

Keranen SV, Kettunen P, Aberg T, Thesleff I, Jernvall J. Gene expression patterns associated with suppression of odontogenesis in mouse and vole diastema regions. Dev Genes Evol. 1999; 209:495–506. [PubMed: 10415326]

Kettunen P, Laurikkala J, Itaranta P, Vainio S, Itoh N, Thesleff I. Associations of FGF-3 and FGF-10 with signaling networks regulating tooth morphogenesis. Dev Dyn. 2000; 219:322–332. [PubMed: 11066089]

Kettunen P, Thesleff I. Expression and function of FGFs-4, -8, and -9 suggest functional redundancy and repetitive use as epithelial signals during tooth morphogenesis. Dev Dyn. 1998; 211:256–268. [PubMed: 9520113]

King MC, Wilson AC. Evolution at two levels in humans and chimpanzees. Science. 1975; 188:107–116. [PubMed: 1090005]

Koenigswald WV, Clemens WA. Levels of complexity in the microstructure of mammalian enamel and their application in studies of systematics. Scanning microscopy. 1992; 6:195–217. discussion 217–198. [PubMed: 1626241]

Li CY, Prochazka J, Goodwin AF, Klein OD. Fibroblast growth factor signaling in mammalian tooth development. Odontology / the Society of the Nippon Dental University. 2014; 102:1–13. [PubMed: 24343791]

Loots GG, Ovcharenko I. rVISTA 2.0: evolutionary analysis of transcription factor binding sites. Nucleic acids research. 2004; 32:W217–221. [PubMed: 15215384]

Mandler M, Neubuser A. FGF signaling is necessary for the specification of the odontogenic mesenchyme. Dev Biol. 2001; 240:548–559. [PubMed: 11784082]

Mathelier A, Zhao X, Zhang AW, Parcy F, Worsley-Hunt R, Arenillas DJ, Buchman S, Chen CY, Chou A, Ienasescu H, et al. JASPAR 2014: an extensively expanded and updated open-access database of transcription factor binding profiles. Nucleic acids research. 2014; 42:D142–147. [PubMed: 24194598]

Portales-Casamar E, Thongjuea S, Kwon AT, Arenillas D, Zhao X, Valen E, Yusuf D, Lenhard B, Wasserman WW, Sandelin A. JASPAR 2010: the greatly expanded open-access database of transcription factor binding profiles. Nucleic acids research. 2010; 38:D105–110. [PubMed: 19906716]

Prud'homme B, Gompel N, Carroll SB. Emerging principles of regulatory evolution. Proceedings of the National Academy of Sciences of the United States of America. 2007; 104(Suppl 1):8605–8612. [PubMed: 17494759]

Rodrigues HG, Merceron G, Viriot L. Dental microwear patterns of extant and extinct Muridae (Rodentia, Mammalia): ecological implications. Die Naturwissenschaften. 2009; 96:537–542. [PubMed: 19127354]

Rodrigues HG, Renaud S, Charles C, Le Poul Y, Sole F, Aguilar JP, Michaux J, Tafforeau P, Headon D, Jernvall J, et al. Roles of dental development and adaptation in rodent evolution. Nat Commun. 2013; 4:2504. [PubMed: 24051719]

Sherf BA. Dual-luciferase reporter assay: an advanced co-reporter technology integrating firefly and Renilla luciferase assays. Promega Notes. 1996; 57:2.

Thesleff I. Epithelial-mesenchymal signalling regulating tooth morphogenesis. Journal of cell science. 2003; 116:1647–1648. [PubMed: 12665545]

Tummers M, Thesleff I. Root or crown: a developmental choice orchestrated by the differential regulation of the epithelial stem cell niche in the tooth of two rodent species. Development. 2003; 130:1049–1057. [PubMed: 12571097]

Visel A, Rubin EM, Pennacchio LA. Genomic views of distant-acting enhancers. Nature. 2009; 461:199–205. [PubMed: 19741700]

Wilson, D.; Reeder, D. Mammal Species of the World. 3. Johns Hopkins University Press; 2005.

Yokohama-Tamaki T, Ohshima H, Fujiwara N, Takada Y, Ichimori Y, Wakisaka S, Ohuchi H, Harada H. Cessation of Fgf10 signaling, resulting in a defective dental epithelial stem cell compartment, leads to the transition from crown to root formation. Development. 2006; 133:1359–1366. [PubMed: 16510502]

A

Brachydont   **Hypsodont**   **Hypselodont**

B
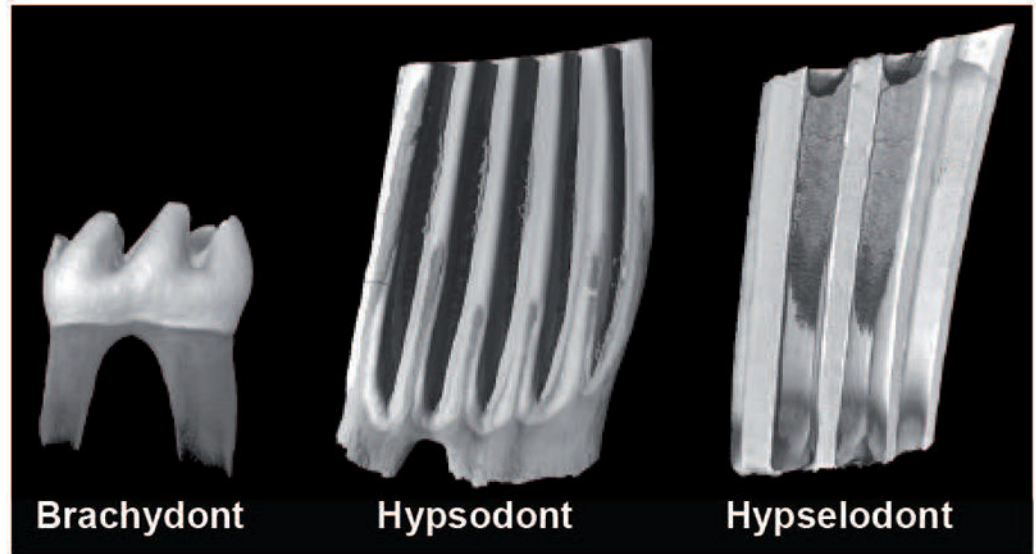
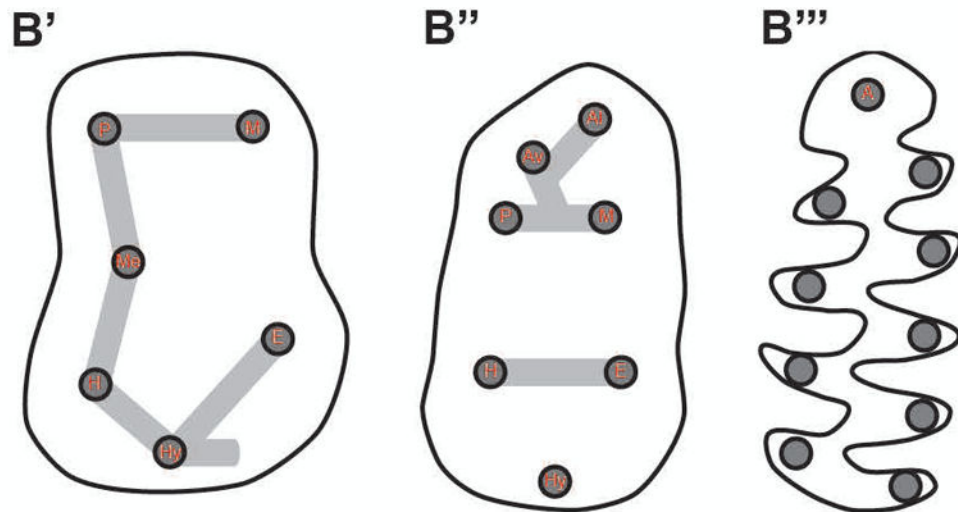**B'**   **B''**   **B'''**

Figure 1.

Schematic representation of dental morphological characters. (A) 3D renderings obtained by X-ray microtomography illustrating three different levels of lower first molar crown height. From left to right: brachydont (*Mus musculus*), hypsodont (*Ondatra zibethicus*), and euhypsodont (*Lemmus lemmus*). (B) Cartoons of occlusal surface organization. From left to right: lower first molar occlusal surface of basal forms, murine rodents (B′ and B″) (including *Mus musculus*), and arvicoline rodents (B‴) (including *Microtus californicus*). Cusp naming abbreviations (in red): P, Protoconid: M, Metaconid; Me, Mesoconid; H, Hypoconid; E, Entoconid: Hy, Hypoconulid; A, Anteroconid; Av, Vestibular anteroconid; Al, Lingual anteroconid. 3D-renderings and cartoons not at scale to facilitate morphological

comparisons. Whereas rounded cusps connected by lophs characterize the murine phenotype, triangular cusps along a main ridge characterize the arvicolin phenotype.
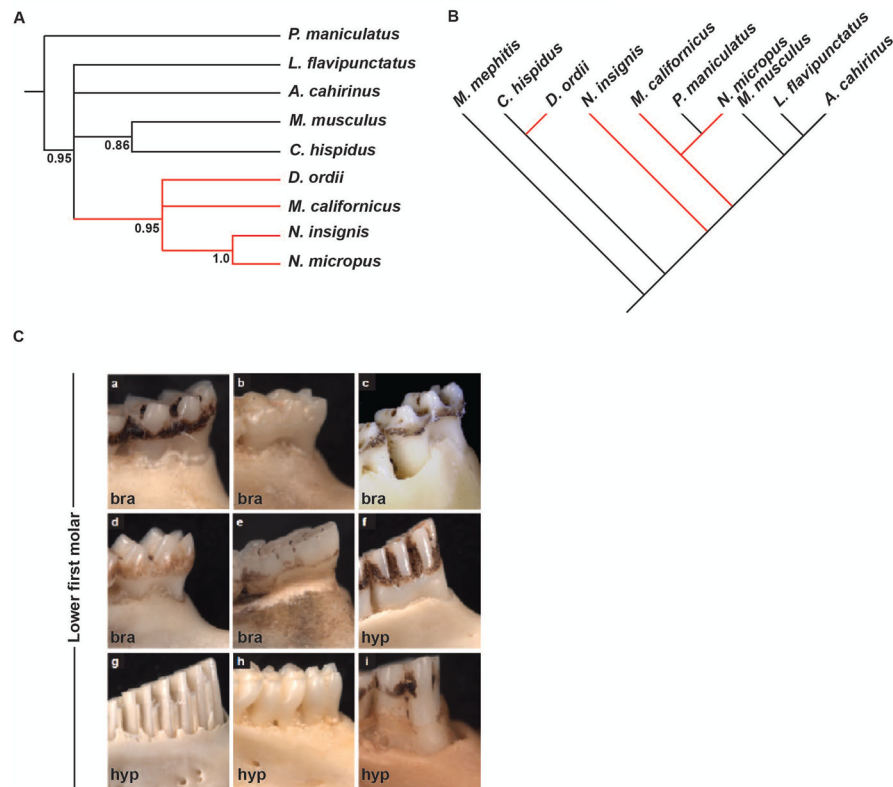
Figure 2.
Molecular phylogeny based on mitochondrial and *Fgf10ECR3* sequence and comparative anatomy based on molar crown/root ratio. (A) Neighbor-joining tree based on *Fgf10ECR3* diversity depicts a single monophyletic clade (red branches) that contains all species with hypsodont molars. (B) Neighbor-joining tree modified from Fabre et al. 2012, depicting phylogenetic relationship based on mitochondrial DNA sequence among all examined species. (C) Buccal view of lower first molar, depicting brachydont (bra) and hypsodont (hyp) phenotypes. a, *Peromyscus maniculatus* (Cricetidae); b, *Mus musculus* (Muridae); c, *Lophuromys flavipunctatus* (Muridae); d, *Acomys cahirinus (*Muridae); e, *Napaeozapus insignis* (Dipodidae); f, *Neotoma micropus* (Cricetidae); g, *Microtus californicus* (Cricetidae); h, *Chaetodipus hispidis* (Heteromyidae); I, *Dipodomys ordii* (Heteromyidae).
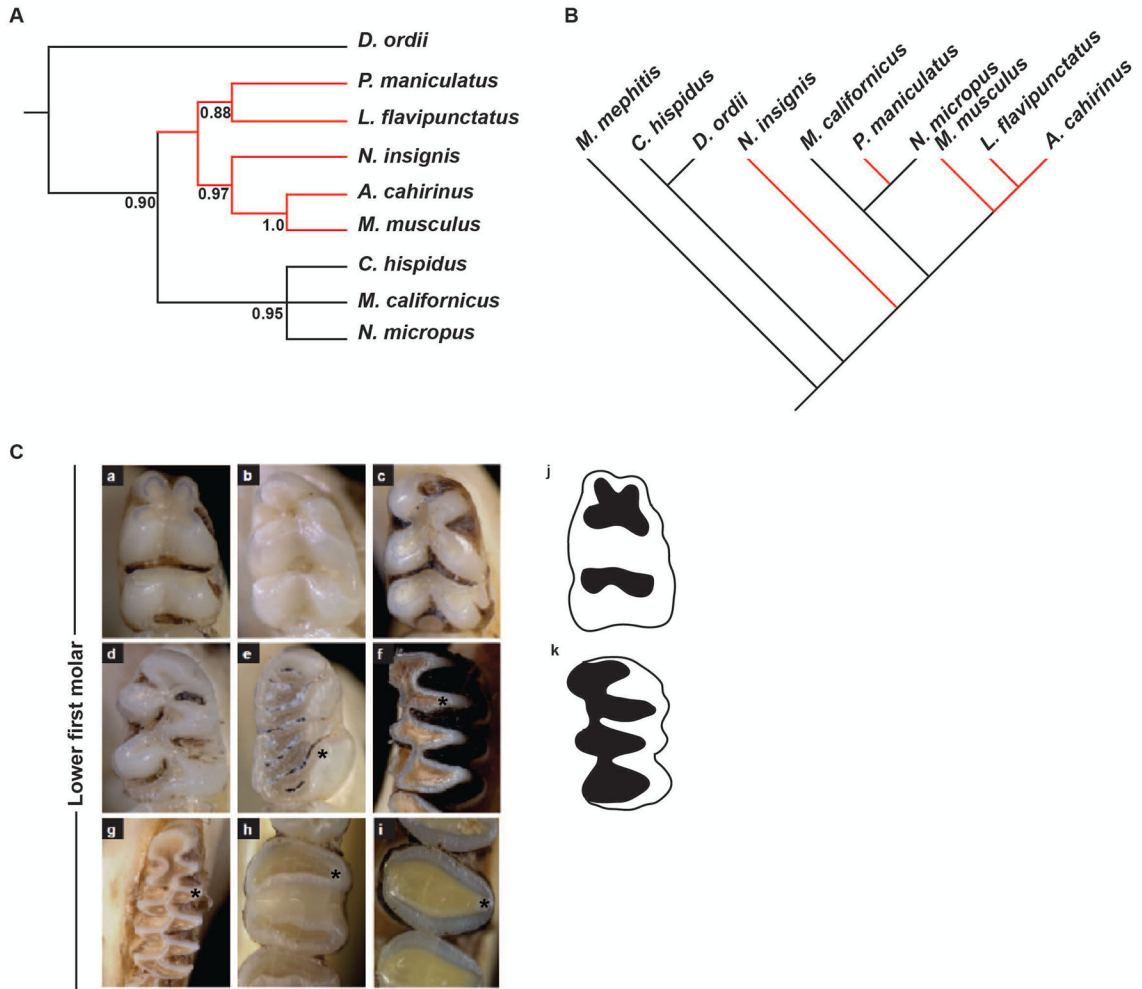
Figure 3.
Molecular phylogeny based on mitochondrial and *Fgf9ECR1* sequence, and comparative anatomy based on lower first molar occlusal view. (A) Neighbor-joining tree based on *Fgf9ECR1* sequence diversity depicts a single monophyletic clade (red branches). (B) Neighbor-joining tree modified from Fabre et al. 2012, depicting phylogenetic relationship based on mitochondrial DNA sequence among all examined species. (C) Occlusal view of lower first molar. Note triangular shape of the cusps in *Microtus californicus* and *Neotoma microtus*. a, *Peromyscus maniculatus*; b, *Mus musculus*; c, *Lophuromys flavipunctatus*; d, *Acomys cahirinus*; e, *Napaeozapus insignis*; f, *Neotoma micropus*; g, *Microtus californicus*; h, *Chaetodipus hispidis*; I, *Dipodomys ordii*; j, graphical representation of a rounded-cusp phenotype; k, graphical representation of a triangular-cusp phenotype.
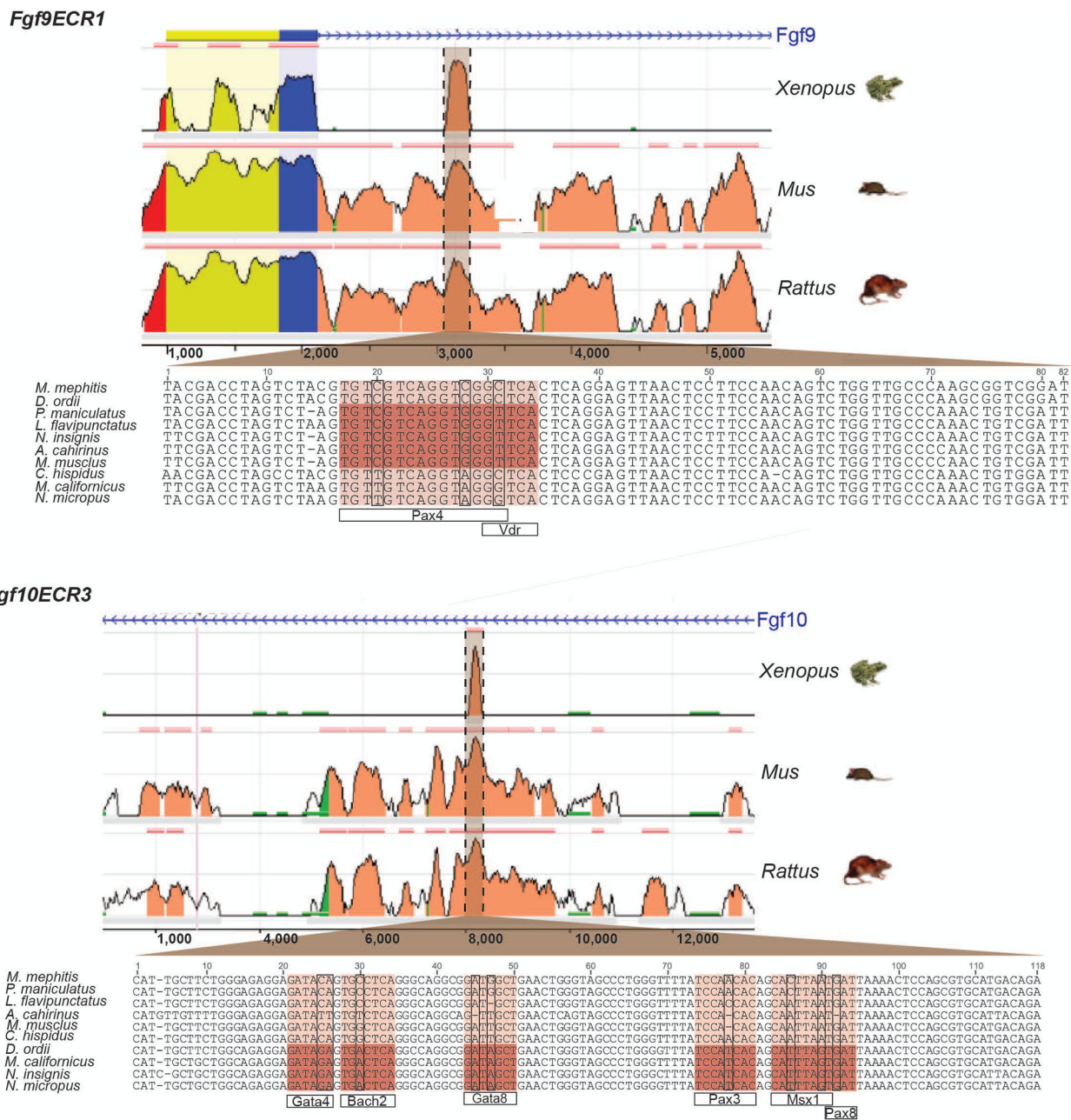
Figure 4.
Identification of *Fgf9ECR1* and *Fgf10ECR3* and TFBS sequence variation. Both *Fgf9ECR1* and *Fgf10ECR3* are located within the first introns of their respective genes. Peak height represents percent sequence identity. Locations of TFBS are highlighted for both ECRs in darker brown.
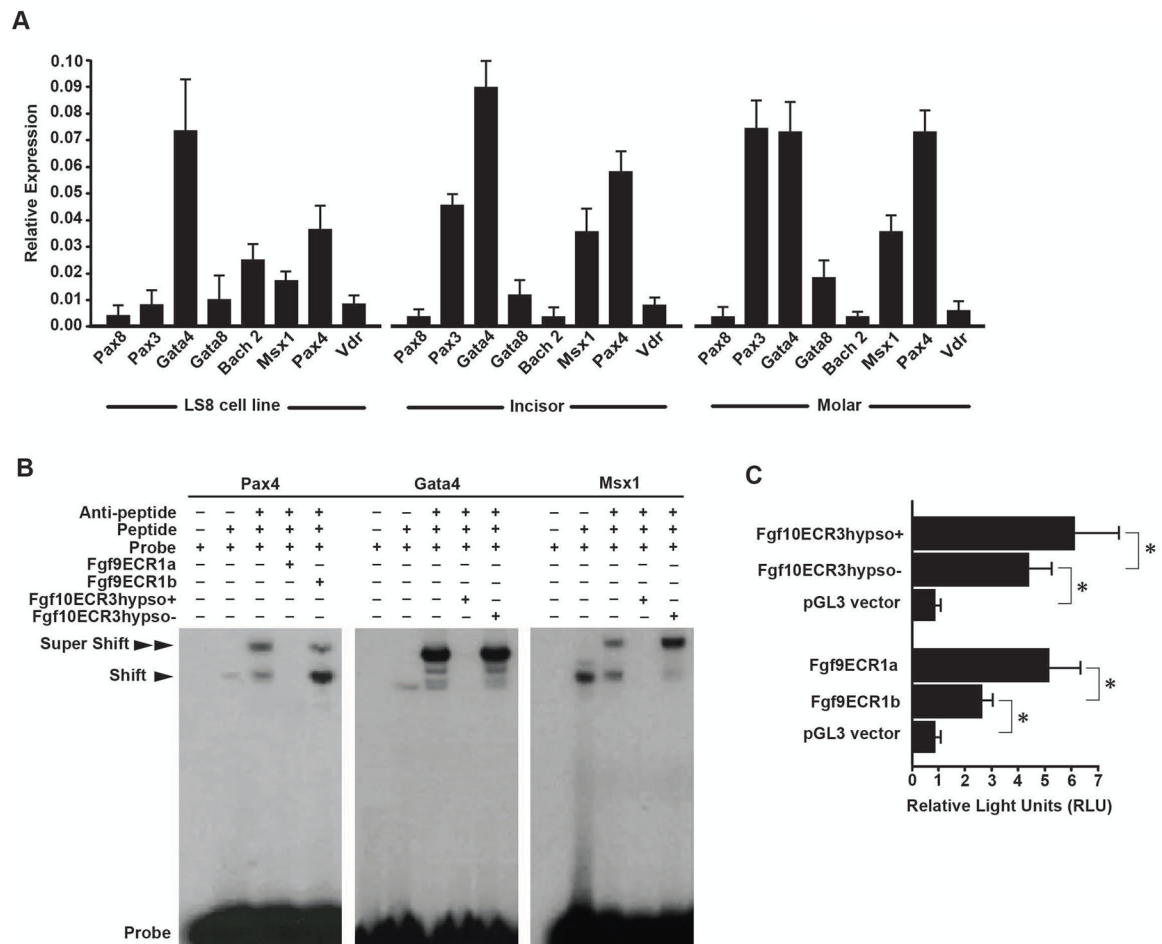
Figure 5.

Analysis of enhancer function of *Fgf9ECR1* and *Fgf10ECR3.* (A) rtPCR expression data of transcription factors associated with the ECRs in LS8 ameloblast cells, adult mouse incisor cervical loops (incisor), and E16.5 mouse molars. (B) EMSA shows that *Fgf9ECR1a* competes with the control probe for interaction with PAX4, and Fgf10ECR3hypso+ competes with the control probe for interaction with MSX1, and GATA4, while *Fgf9ECR1b* and *Fgf10ECR3hypso–* do not. (C) Luciferase assay conducted in LS8 cells shows stronger enhancer function in *Fgf9ECR1a* and *Fgf10ECR3hypso+* than *Fgf9ECR1b* and *Fgf10ECR3hypso–* (*p<0.001).